

LETTERS

A common somitic origin for embryonic muscle progenitors and satellite cells

Jérôme Gros¹, Marie Manceau¹, Virginie Thomé¹ & Christophe Marcelle¹

In the embryo and in the adult, skeletal muscle growth is dependent on the proliferation and the differentiation of muscle progenitors present within muscle masses. Despite the importance of these progenitors, their embryonic origin is unclear^{1,2}. Here we use electroporation of green fluorescent protein in chick somites³, video confocal microscopy analysis of cell movements, and quail–chick grafting experiments to show that the dorsal compartment of the somite, the dermomyotome, is the origin of a population of muscle progenitors that contribute to the growth of trunk muscles during embryonic and fetal life. Furthermore, long-term lineage analyses indicate that satellite cells, which are known progenitors of adult skeletal muscles⁴, derive from the same dermomyotome cell population. We conclude that embryonic muscle progenitors and satellite cells share a common origin that can be traced back to the dermomyotome.

During early somite differentiation, muscle growth in the trunk is entirely dependent on the generation of post-mitotic myocytes emanating from the four borders of the epithelial dermomyotome to form the primary myotome⁵. However, the dermomyotome is a transient structure that progressively disappears during development^{6,7} (Fig. 1a–c); this type of muscle formation therefore cannot account for the continuous and intense growth of muscles observed during late embryonic and fetal life, long after the dermomyotome has disappeared. Muscle progenitors, giving rise to muscles in culture and *in vivo*, and expressing early skeletal muscle markers, have been identified in all skeletal muscles of amniote embryos⁸. However, the timing and the developmental process through which they appear within the muscle masses are unknown.

In the adult, muscle growth and repair rely on the proliferation and the differentiation of satellite cells, located under the basal lamina of muscle fibres and recognized by their expression of specific molecular markers (such as the paired box transcription factor Pax7) (ref. 9). The embryonic origin of these satellite cells is unclear. Early experiments using the quail–chick chimera technique suggested a somitic origin¹⁰; however, this work did not identify the progenitor cell types at the origin of satellite cells or the developmental route that they followed to differentiate into satellite cells. More recently, alternative origins have been proposed for satellite cells, including cells derived from blood vessel walls (such as the aorta) and bone marrow cells, thus supporting a model where satellite cell development could take place independently of somitic myogenesis^{9,11–13}.

To identify the origin of embryonic muscle progenitors and satellite cells, we traced the fate of dermomyotome cells from the early stages of somite differentiation through to hatching. The early dermomyotome has an epithelial morphology; as somites mature, it undergoes a progressive epithelial–mesenchymal transition (EMT)¹⁴, which is characterized by the loss and/or the relocalization of the epithelial markers N-cadherin, β -catenin and F-actin at the adherens junctions located at the apical end of dermomyotomal

cells (Fig. 1a–l). The EMT of the dermomyotome is thought to be the first step in dermis formation¹⁵, and precedes the dorsal-ward migration of dermis progenitor cells from the somite towards the ectoderm.

Concomitant with the EMT, we observed a dramatic increase in the number of BrdU-positive cells within the myotome (Fig. 1m–p), suggesting that the EMT of the dermomyotome triggers the emergence of a proliferative cell population in the myotome, probably emanating from the dermomyotome. To verify this, we used electroporation of green fluorescent protein (GFP) to follow the movements of cells originating from the central region of the dermomyotome (Fig. 2a). Thirty-six hours after electroporation, as the EMT of the dermomyotome is initiated, a few GFP-positive cells were found within the myotome (Fig. 2b). As the incubation time increased, we observed a massive entry of GFP-positive cells emanating from the dermomyotome (Fig. 2c, e). This process was not uniform along the medio-lateral axis of the somite: in the lateral domain of the dermomyotome, all GFP-positive cells readily entered the myotome (L in Fig. 2c). In contrast, in the medial domain (M in Fig. 2c), most GFP-labelled cells remained dorsal to the primary myotome. However, by embryonic day (E)7.5 (120 h after electroporation) the medial domain was intensely GFP-labelled (Fig. 2f). This could be due to late entry of GFP-labelled cells from the dorso-medial dermomyotome or to intense proliferation of the few GFP-positive cells observed in this region before E7.5. When small regions of the dermomyotome were electroporated, the relative positions of GFP-positive cells within the myotome corresponded roughly to their original positions within the dermomyotome, indicating that little migration of dermomyotome-derived cells occurred within the plane of the myotome (not shown). This confirms previous data obtained using the quail–chick grafting technique^{15,16}. Many GFP-positive cells never entered the primary myotome, but remained between this structure and the ectoderm, presumably giving rise later to the development of dorsal dermis¹⁵ (arrowheads in Fig. 2d–f).

To determine the route that dermomyotomal cells take to enter the primary myotome, we used an *ex vivo* embryo-slice culture system combined with confocal time-lapse videomicroscopy. In contrast to what had been observed during primary myotome formation⁵, dermomyotomal cells did not transit across the dermomyotome borders; rather, they translocated directly from the central dermomyotome into the myotome (Fig. 2g–i). Real-time observation of this process (see Supplementary Video) revealed several additional features. First, a cell division preceded the translocation (Fig. 2h). Second, the plane of division was perpendicular to the apico-basal axis of the mother cell. Finally, the cytokinesis process was very rapid (6–12 min) and resulted in the translocation of one of the daughter cells into the myotome, while the other daughter remained in the dermomyotome (Fig. 2i).

We analysed the molecular characteristics of this population of

¹Laboratoire de Génétique et de Physiologie du Développement, Developmental Biology Institute of Marseille, CNRS UMR 6545, Université de la Méditerranée, Campus de Luminy, case 907, 13288 Marseille Cedex 09, France.

cells as they entered the myotome, as well as their fate during embryonic development. Twelve hours after initiation of the dermo-myotome EMT (that is, 48 h after somite formation), 90% of GFP-positive cells present in the primary myotome expressed the early muscle progenitor cell marker Pax7. These GFP-positive cells were actively dividing (as shown by BrdU immunoreactivity) and only a

small percentage (10%) expressed the differentiated muscle marker myosin heavy chain (MyHC) (Fig. 3b and Supplementary Fig. 1a, d). As development proceeded, we observed a continuous increase in the contribution of the GFP-positive cell population to the differentiated muscle masses (shown by a gradual increase in MyHC/GFP double staining), while a portion of the GFP-positive cells (25% at E7.5)

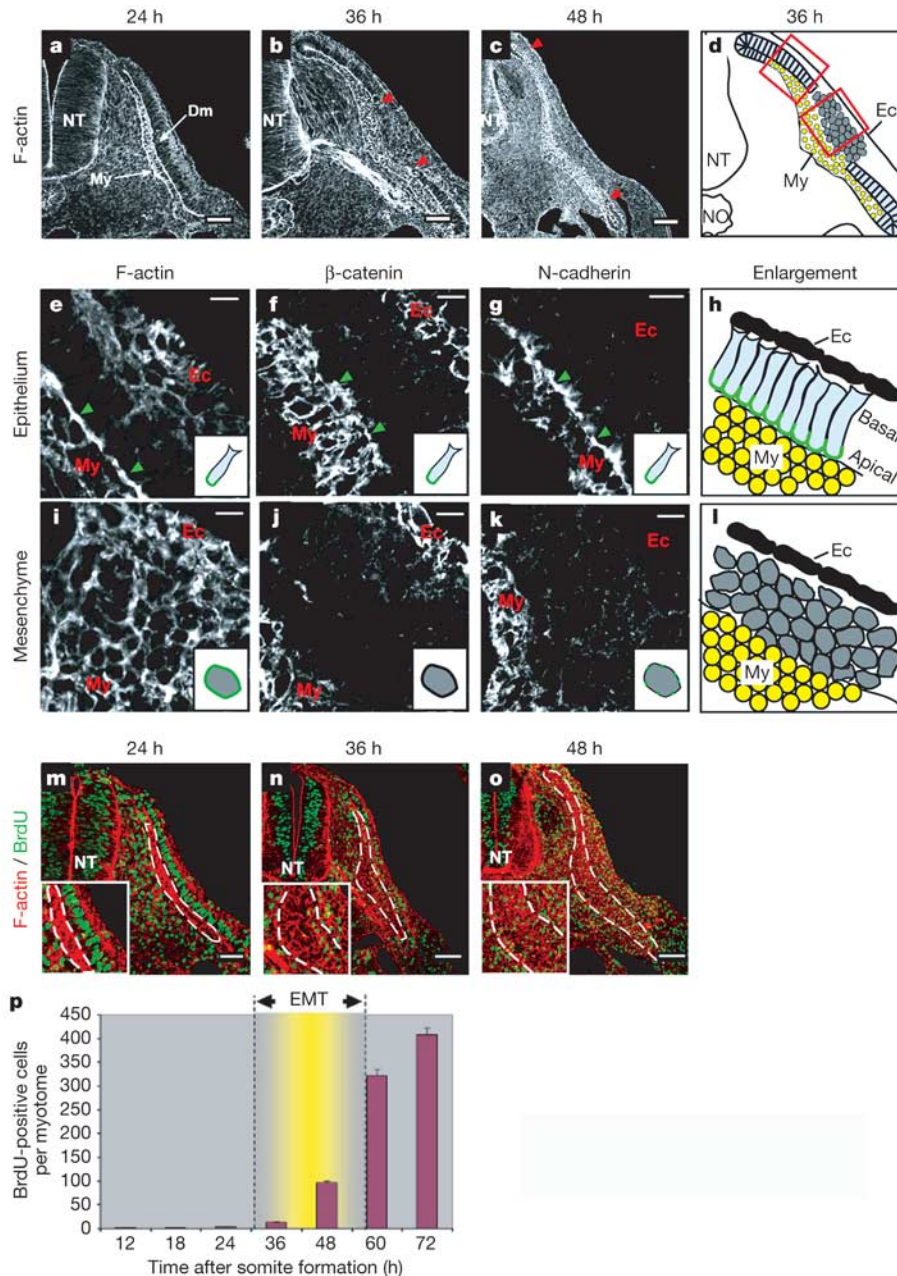


Figure 1 | The EMT of the dermo-myotome triggers the emergence of a BrdU-positive cell population in the myotome. **a–c**, Confocal optical slices of somites (somite number 23), stained for F-actin 24 h (**a**), 36 h (**b**) or 48 h (**c**) after somite formation. NT, neural tube. **a**, At 24 h, the dermo-myotome (Dm) is epithelial. **b, c**, Between 24 and 36 h, the central region of the dermo-myotome begins a de-epithelialization process (red arrowheads in **b** and **c**) that progresses medially and laterally as development proceeds. **e–g** and **i–k**, Enlargements of sections through the epithelial (**e–g**) and the mesenchymal (**i–k**) regions of a dermo-myotome, 36 h after somite formation (as shown in **b** and **d**). The regions shown in **e–g** and **i–k** correspond to the boxed areas in **d**, enlarged in **h** and **l**. Epithelial cells express F-actin (**e**, see also inset in Fig. 2a), β -catenin (**f**), and N-cadherin (**g**) at their apical end (green arrowheads and insets in **e–g**). The myotome (My)

expresses all three molecules, and the ectoderm (Ec) stains for F-actin and β -catenin. During EMT, the apical staining of all three markers is lost. F-actin relocates evenly in the cells (**i**, inset), overall β -catenin staining is reduced (**j**, inset) and N-cadherin staining becomes punctated (**k**, inset). **m–o**, Representative sections of interlimb somites stained for F-actin (in red) and BrdU (in green) to distinguish the myotome (highlighted with dotted lines) before (**m**) and during (**n, o**) the EMT. The myotome is devoid of BrdU-positive cells before EMT (**m** and inset) but a sharp increase in BrdU staining occurs at the time of the EMT (**n, o** and insets). **p**, Cell count of BrdU-positive cells within the myotome of a somite 12–72 h after its formation. Cell counts were performed on 12–15 sections per time point (>12,000 BrdU-positive cells counted); error bars show standard deviation. Scale bars, 50 μ m (**a–c, m, n**), 10 μ m (**e–k**), 100 μ m (**o**).

maintained early muscle progenitor characteristics (that is, Pax7 expression) and BrdU immunoreactivity during embryonic development (Fig. 3b and Supplementary Fig. 1b, c, e, f). Together, these data demonstrate that the cell population emerging from the dermomyotome as it undergoes an EMT contains embryonic muscle progenitors.

We next determined whether all embryonic muscle progenitors present in the myotome derive from the central region of the dermomyotome. A limitation of the electroporation technique is that it does not result in transfection of all targeted cells (in the best cases, 50% of the cells are electroporated, data not shown). Thus, the answers obtained using electroporation are more qualitative than truly quantitative. In contrast, the quail–chick grafting technique is particularly suitable for addressing this question, because we can use a marker of quail cells (the quail cell perinuclear antigen or QCPN) to

follow a population of grafted quail cells within a chick host during embryonic development.

We replaced the central region of the dermomyotome of four consecutive chick somites with central dermomyotome from quails (Fig. 3c). After a 24-h reincubation, we verified that the central dermomyotome was of quail origin (recognized by a QCPN quail-specific antibody), but that the dermomyotome borders were of chick origin (Supplementary Fig. 1g, h). After 48 h, quail dermomyotome cells entered the QCPN-negative, chick-derived primary

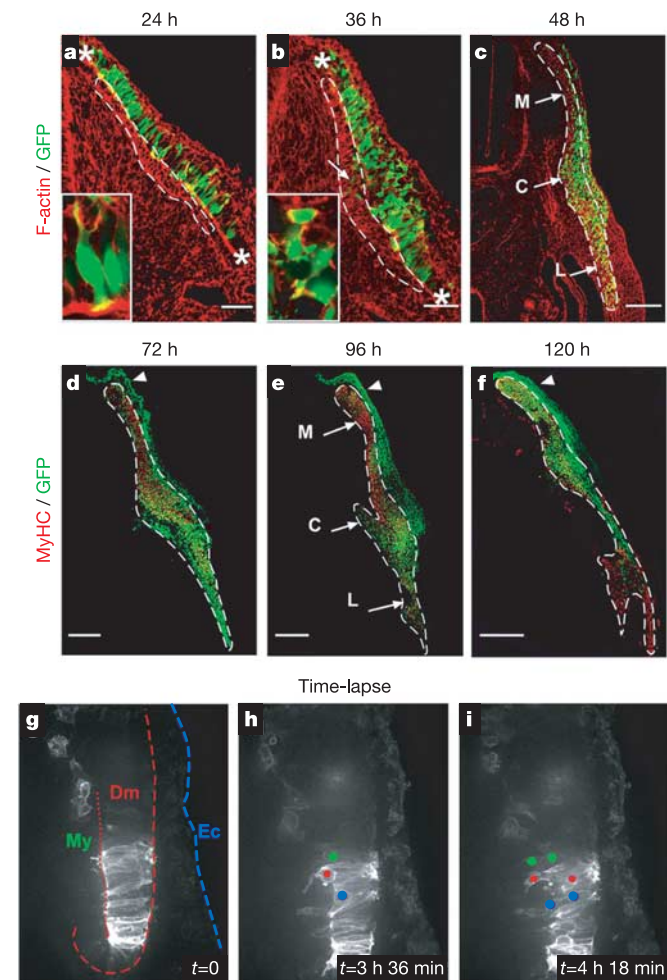


Figure 2 | Direct translocation of dermomyotome cells into the primary myotome. **a–f**, Sections of somites electroporated with GFP (medial and lateral borders indicated by white asterisks in **a**, **b**). **b**, 36 h after somite formation, a few GFP-positive cells (arrow) enter the primary myotome. **c–f**, After 48 h, many GFP-positive cells have entered the primary myotome. The dynamics of the distribution of GFP-positive cells is different in the lateral (L), central (C) and medial (M) domains. Insets in **a** and **b** show the morphological difference between epithelial (**a**) and mesenchymal (**b**) dermomyotome cells. **g–i**, Time-lapse confocal analysis (see Supplementary Video) showing the direct translocation of dermomyotome (Dm) cells into the myotome (My). Ec, ectoderm. 36 h after electroporation, somites were examined in an *ex vivo* embryo-slice culture system. Images in **h** and **i** show the cell division and translocation of three cells (coloured) from the dermomyotome into the myotome. Scale bars, 50 μm (**a**, **b**) 200 μm (**c**, **d**), 400 μm (**e**), 500 μm (**f**).

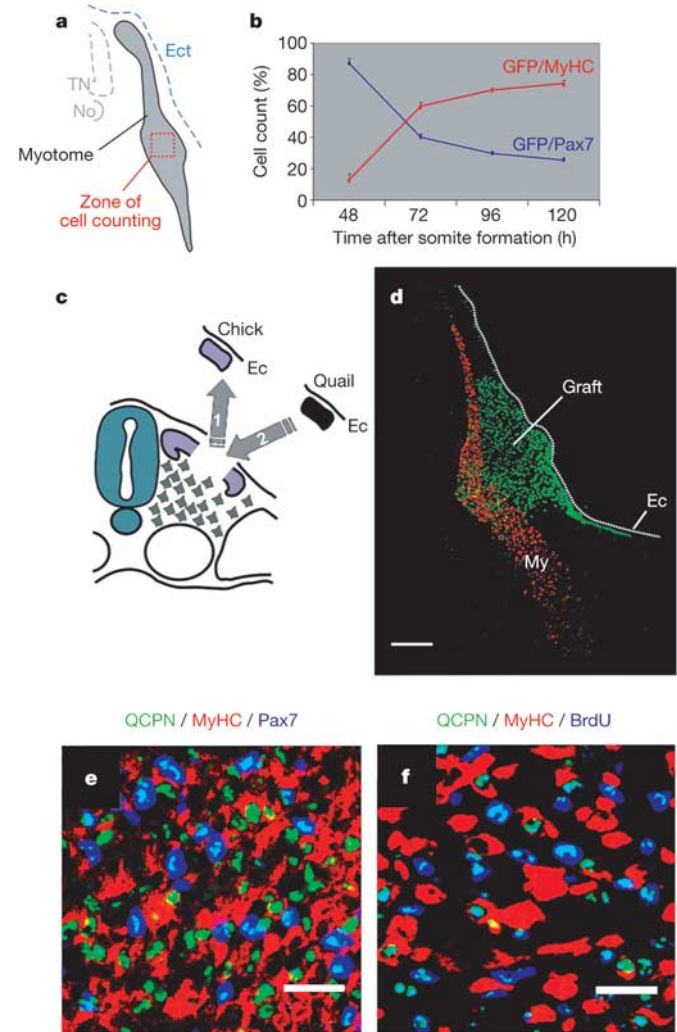


Figure 3 | Dermomyotome-derived cells contribute to embryonic muscle growth. Somites electroporated in the central dermomyotome were analysed 48–120 h after electroporation (data shown in Supplementary Fig. 2a–e). We counted the number of cells staining for either GFP + Pax7 or GFP + MyHC in a region corresponding to a central domain of the myotome (red dotted square in **a**). **b**, The contribution of the muscle progenitor population to muscle growth. Cell counts are expressed as a percentage of the GFP-positive cells in the entire myotome (counted zone delineated in **a**). For each time point, 12–15 sections were counted (>5,500 cells in total); error bars indicate standard deviation. Most GFP-positive cells expressed Pax7 48 h after electroporation. As development proceeds, a growing number of cells initiate MyHC expression. We did not observe any cells staining for both Pax7 and MyHC. At all stages, a small proportion of cells (about 5%) were neither Pax7- nor MyHC-positive. **c**, A schematic of the quail–chick grafting experiments. **d**, Section from a chimaera analysed 72 h after grafting. In the region of the graft, numerous QCPN-positive quail cells (green) are seen within the myotome (red). **e**, **f**, Within the myotome of the embryo shown in **d**, most BrdU-positive (blue in **e**) or Pax7-positive (blue in **f**) cells express the QCPN antigen, observed as an irregular blue-green staining in the nuclei. Scale bars, 200 μm (**d**), 10 μm (**e**, **f**).

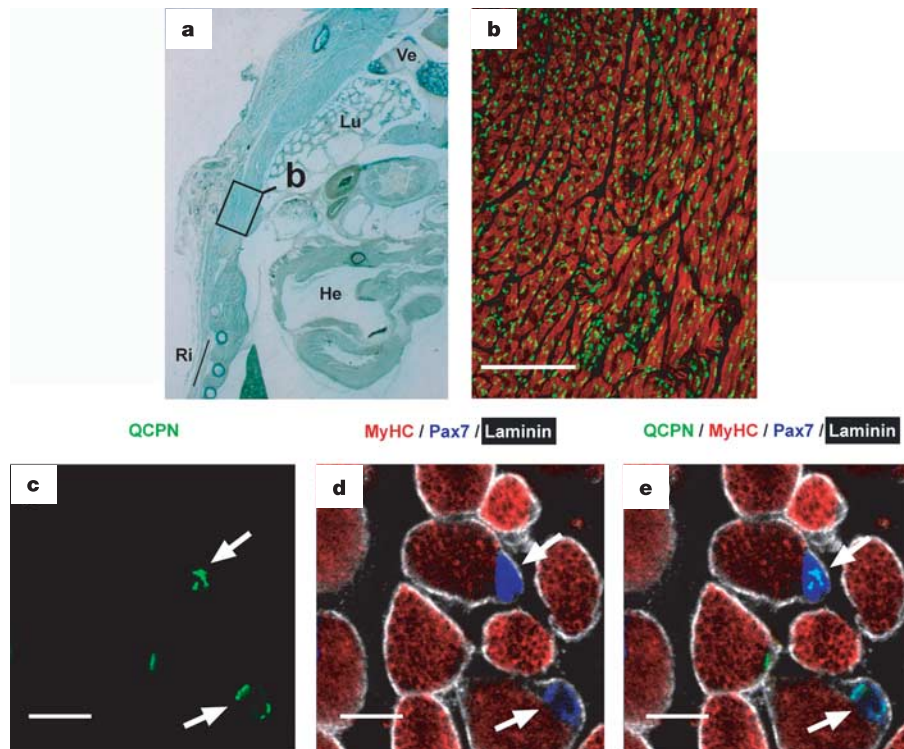


Figure 4 | Satellite cells are derived from the dermomyotome. **a**, Histological view (light green staining) of a post-hatch quail–chick chimaera. Ve, vertebra; He, heart; Ri, rib; Lu, lung. **b**, Confocal view of the zone delineated in **a**, stained for MyHC (red) and the quail marker QCPN (green). The muscle is markedly colonized by quail cells. **c–e**, Confocal

images showing quadruple staining with antibodies against QCPN (green), MyHC (red), Pax7 (blue) and laminin (white). Quail (Pax7-positive) cells located under the basal lamina (arrows) identify satellite cells. Scale bars, 100 μm (**b**), 5 μm (**c–e**).

myotome (Supplementary Fig. 1i, j). After 72 h we observed, in the region of the graft, that the vast majority of Pax7-positive (97%) or BrdU-positive (93%) cells within the myotome stained for the quail marker (Fig. 3d–f). This suggests that most, if not all, proliferative embryonic muscle progenitors present in the myotome at that stage of development derive from the central dermomyotome. In a complementary experiment, we observed that the borders of the dermomyotome do not generate cells with characteristics of embryonic muscle progenitors, even after a long (7-day) reincubation period (Supplementary Fig. 2a–e), confirming that the contribution of the epithelial dermomyotome borders to the population of embryonic muscle progenitors is negligible.

We next determined whether a portion of dermomyotomal cells maintain myogenic potential into late fetal life and after hatching. In chick, it has been shown that cells with satellite cell characteristics appear within muscle masses during late fetal life, between E15 and E17 of development^{4,10,17,18}. At E18, satellite cells constitute the majority (about 85%) of the population of muscle progenitors, and at hatching (E21 in chick) they represent virtually all progenitors present in the muscle masses^{4,10,17,18}. Satellite cells are traditionally identified by their localization between the muscle fibre and the basal lamina¹⁹; however, Pax7 has recently been used as a reliable satellite cell marker. Using these two criteria, we determined whether we could identify, in late fetal life, satellite cells derived from the dermomyotome. Embryos were electroporated as described above and left to develop until late fetal life. In addition to GFP-labelled muscle fibres at E18, we found GFP-labelled, Pax7-positive cells tightly associated with muscle fibres and localized between the MyHC-positive muscle fibre and the laminin-positive basal lamina—a position that characterizes satellite cells (Supplementary Fig. 3a–d). As the GFP marker gradually becomes diluted with cell division, few GFP-positive satellite cells could be observed at E18. In

contrast, owing to the stability of the quail marker, we have been able to quantify the results obtained for the chimaeras. In the region of the graft, in E18 as well as in post-hatching chimaeras (Fig. 4a, d and Supplementary Fig. 3e–h), we found that 91% (E18) and 95% (post-hatch) of the satellite cells were of quail origin (cell count, $n = 600$ total in 4 specimens). A minor fraction of satellite cells could not be identified as quail, possibly owing to alternative origins of these cells or a limitation of the identification technique in quail cells (not all are recognized by the QCPN antibody, even in a bona fide quail; data not shown). Taken together, our data strongly suggest that most satellite cells present in skeletal muscles of the trunk derive from the central region of the dermomyotome.

In summary, our use of electroporation, *ex vivo* analyses of cell movements and the quail–chick grafting technique, has allowed us to analyse the morphogenesis and growth of skeletal muscles in birds. Our analyses have revealed that myogenesis follows two distinct stages. In the first stage of myotome morphogenesis, the epithelial borders of the dermomyotome generate postmitotic myocytes that readily organize into a primary myotome⁵. The second stage of myotome growth, described in the present work, is dependent on the emergence of a population of muscle progenitors within the primary myotome, triggered by the EMT of the dermomyotome. At a cellular level, the mode of cell translocation in the first and the second stages are clearly distinct. During the first stage of myotome morphogenesis, single cells translocate into the myotome while their neighbours remain epithelial. In the second stage, the epithelial integrity of the dermomyotome is disrupted before or concomitant with cell translocation. Notably, this change is correlated with the formation of dramatically different cell types (postmitotic myocytes versus proliferative muscle progenitors).

Finally, our approaches have allowed the characterization of the developmental route that leads to the emergence of satellite cells.

Previous studies had questioned the somitic origin of satellite cells by demonstrating that bone-marrow-derived cells can give rise, under specific experimental conditions, to satellite cells as well as muscle fibres. Recent work has shown that in adults, the satellite cell pool does not receive any significant haemopoietic input²⁰. Our data show that under normal developmental conditions, the vast majority, if not all, satellite cells are derived from the dermomyotome.

In conclusion, the demonstration of a common origin for embryonic muscle progenitors and satellite cells in amniotes opens new avenues for studying their roles in muscle growth and repair, and may lead to insights of therapeutic value.

METHODS

Electroporation. Newly formed epithelial somites were electroporated as previously described^{3,5}. In all cases, thoraco-lumbar (that is, interlimb) somites were electroporated. The positive and negative electrodes were positioned so that the dorsal region of somites (which gives rise to the dermomyotome) was electroporated. Embryos were screened by ultraviolet light examination one day after electroporation, and only embryos in which the central region of the dermomyotome was electroporated were kept for further analyses. A cytoplasmic form of GFP was used in all but the time-lapse experiment, for which a membranous form of GFP was used.

Antibodies, immunohistochemistry and confocal analysis. Phalloidin Alexa 456 (Molecular Probes) was used to detect F-actin. The following antibodies were used: mouse monoclonal antibodies against β -catenin (Transduction Laboratories), N-cadherin (C-8538, Sigma), BrdU (Becton-Dickinson), Pax7 (Hybridoma Bank), Light Meromyosin (MF20, Hybridoma Bank), GFP (Molecular Probes), QCPN (Hybridoma Bank); a rat monoclonal antibody against BrdU (Abcam); polyclonal antibodies against laminin (L-9393, Sigma) and GFP (Torrey Pines Biolabs). To analyse cell division, embryos were exposed to BrdU for 1 h. For simultaneous detection of 4 antigens by indirect fluorescence (Fig. 4d–f), spectral deconvolution was used. This was accomplished using a Zeiss confocal microscope (LSM 510 Meta). To identify satellite cells in pre-hatching chick embryos, 6 embryos electroporated at E3 were analysed at E18. In 4 of the 6 embryos, GFP-positive muscle fibres were found in the muscle masses. GFP-positive satellite cells were clearly identified in 3 out of the 4 embryos (see Fig. 4).

Time-lapse analysis. To observe the translocation movement of dermomyotome cells into the myotome, we used an *ex-vivo* embryo-slice culture system combined with confocal time-lapse videomicroscopy. Embryo slices (200–250- μ m thick) of the trunk region were placed in a 3-cm Petri dish in which the bottom had been replaced with a glass coverslip. Low-melting-point agarose (1%) in F-12 nutrient mixture (Ham) was poured around and above the embryo slice. The sample was placed in a heated chamber and examined on an inverted microscope (Axiovert, Zeiss) to which a Nipkow spinning disk confocal head (UltraView, Perkin Elmer) was attached. Embryo slices can be kept in this culture system for at least 24 h. Metamorph image acquisition software was used to drive the microscope and the confocal head. Confocal stacks were taken at 6-min intervals.

Quail–chick grafting. We replaced the central region of the dermomyotome of 4 consecutive interlimb chick somites with central dermomyotome from quail. The surgeries were performed in differentiated somites (for example, somite stage IV–VII in a 30-somite chick embryo) with glass needles, taking care not to transplant the dermomyotome borders. The ectoderm was grafted together with the four pieces of dermomyotome attached to it. Embryos were analysed after 24 h ($n = 15$), 48 h ($n = 13$) and 72 h ($n = 10$). For long-term lineage analyses, we generated 84 quail–chick chimaeras, of which 13 reached the end of fetal life, 2 embryos were analysed at E18 and 2 chimaera were analysed after hatching.

Received 4 February; accepted 23 March 2005.

Published online 20 April 2005.

1. Morgan, J. E. & Partridge, T. A. Muscle satellite cells. *Int. J. Biochem. Cell Biol.* **35**, 1151–1156 (2003).
2. Parker, M. H., Seale, P. & Rudnicki, M. A. Looking back to the embryo: defining transcriptional networks in adult myogenesis. *Nature Rev. Genet.* **4**, 497–507 (2003).
3. Scaal, M., Gros, J., Lesbros, C. & Marcelle, C. In ovo electroporation of avian somites. *Dev. Dyn.* **229**, 643–650 (2004).
4. Mauro, A. Satellite cell of skeletal muscle fibers. *J. Biophys. Biochem. Cytol.* **9**, 493–495 (1961).
5. Gros, J., Scaal, M. & Marcelle, C. A two-step mechanism for myotome formation in chick. *Dev. Cell* **6**, 875–882 (2004).
6. Christ, B. & Ordahl, C. P. Early stages of chick somite development. *Anat. Embryol. (Berl.)* **191**, 381–396 (1995).
7. Scaal, M. & Christ, B. Formation and differentiation of the avian dermomyotome. *Anat. Embryol. (Berl.)* **208**, 411–424 (2004).
8. Hauschka, S. in *Myology* (eds Engel, A. & Franzini-Armstrong, C.) 3–74 (McGraw-Hill, New York, 1994).
9. Seale, P., Asakura, A. & Rudnicki, M. A. The potential of muscle stem cells. *Dev. Cell* **1**, 333–342 (2001).
10. Armand, O., Boutineau, A. M., Mauger, A., Pautou, M. P. & Kiény, M. Origin of satellite cells in avian skeletal muscles. *Arch. Anat. Microsc. Morphol. Exp.* **72**, 163–181 (1983).
11. De Angelis, L. *et al.* Skeletal myogenic progenitors originating from embryonic dorsal aorta coexpress endothelial and myogenic markers and contribute to postnatal muscle growth and regeneration. *J. Cell Biol.* **147**, 869–878 (1999).
12. Ferrari, G. *et al.* Muscle regeneration by bone marrow-derived myogenic progenitors. *Science* **279**, 1528–1530 (1998).
13. Gussoni, E. *et al.* Dystrophin expression in the *mdx* mouse restored by stem cell transplantation. *Nature* **401**, 390–394 (1999).
14. Tosney, K. W., Dehnbostel, D. B. & Erickson, C. A. Neural crest cells prefer the myotome's basal lamina over the sclerotome as a substratum. *Dev. Biol.* **163**, 389–406 (1994).
15. Olivera-Martinez, I., Coltey, M., Dhoulailly, D. & Pourquié, O. Mediolateral somitic origin of ribs and dermis determined by quail–chick chimeras. *Development* **127**, 4611–4617 (2000).
16. Huang, R. & Christ, B. Origin of the epaxial and hypaxial myotome in avian embryos. *Anat. Embryol. (Berl.)* **202**, 369–374 (2000).
17. Feldman, J. L. & Stockdale, F. E. Temporal appearance of satellite cells during myogenesis. *Dev. Biol.* **153**, 217–226 (1992).
18. Hartley, R. S., Bandman, E. & Yablonka-Reuveni, Z. Skeletal muscle satellite cells appear during late chicken embryogenesis. *Dev. Biol.* **153**, 206–216 (1992).
19. Bischoff, R. in *Myology* (eds Engel, A. & Franzini-Armstrong, C.) 97–119 (McGraw-Hill, New York, 1994).
20. Sherwood, R. I. *et al.* Isolation of adult mouse myogenic progenitors: functional heterogeneity of cells within and engrafting skeletal muscle. *Cell* **119**, 543–554 (2004).

Supplementary Information is linked to the online version of the paper at www.nature.com/nature.

Acknowledgements We thank K. Tosney for discussions on the process of dermomyotome EMT, and O. Pourquié, T. Lecuit, S. Kerridge and U. Rothbacher for comments on the manuscript. We acknowledge the help of C. Moretti and P. Weber from the Institute's Imaging Facility and of the Zeiss team. This study was funded by grants from the Actions Concertées Incitatives, the Association Française contre les Myopathies and by the EEU 6th Framework Programme Network of Excellence MYORES. J.G. and M.M. are Fellows from the Ministère de la Recherche et des Technologies.

Author Information Reprints and permissions information is available at npg.nature.com/reprintsandpermissions. The authors declare no competing financial interests. Correspondence and requests for materials should be addressed to C.M. (marcelle@ibdm.univ-mrs.fr).